JOURNAL OF MATERIALS SCIENCE 18 (1983) 1765–1772

Fracture of LiF bicrystals

JONG Y. LEE, K. N. SUBRAMANIAN
Department of Metallurgy, Mechanics and Materials Science, Michigan State University, East Lansing, Michigan 48824, USA

The role of relative crystallographic orientation and grain boundary orientation on crack propagation in LiF bicrystals was investigated by using LiF bicrystals grown by the Czochralski method. Constant compliance specimens were fractured by driving a wedge through notched specimens, and the fracture load was measured using a calibrated load cell. The direction of crack propagation was dictated according to the misorientation angles, and the fracture load was observed to increase as the misorientation angles increased.

1. Introduction

In crystalline materials, fracture may occur by either transcrystalline cleavage or intercrystalline fracture. There are many factors that affect the fracture mode such as temperature, loading method, grain size, crystal structure, alloying elements, test environment, and relative crystallographic orientations [1–7]. In this work the role of relative crystallographic orientation and grain boundary orientation with respect to the crack path on fracture was studied to gain a better understanding of the fundamental mechanism of crack propagation in polycrystalline materials. Bicrystals of LiF were used as model specimens for this investigation, since LiF has a simple crystal structure, well defined slip systems and cleavage planes. LiF has a rock-salt structure. The primary and secondary slip planes are {1 1 0} and {1 0 0}, respectively. The slip directions are $\langle 1\,\bar{1}\,0\rangle$ in both systems [8, 9]. The primary and secondary cleavage planes are {1 0 0} and {1 1 0}, respectively. In LiF single crystal, at room temperature, fracture normally occurs by primary cleavage.

Cracks can move as fast as 2000 m sec^{-1} along {1 0 0} planes in LiF crystals [10]. This maximum, or terminal, velocity is limited by the inertia of the crystal as it opens up to form the crack. At crack velocities near the terminal value, there is no time for dislocation nucleation; but at a much lower velocity (about 60 m sec^{-1}) dislocation loops begin to form in front of a crack tip [10, 11]. At velocities less than about half the critical velocity, enough plastic flow occurs to make crack propagation unstable [10].

2. Experimental procedure

Lithium fluoride bicrystals were grown by the Czochralski method using two LiF single crystal seeds in an argon atmosphere. The seed setting used is shown in Fig. 1. To change the misorientation angles, one seed (seed A) was rotated by an angle ϕ keeping its (0 0 1) plane to remain perpendicular to the crystal growth direction. The bicrystals grown also have a constant tilt angle (α) of 45° since one of the seeds (seed B) was kept tilted at 45°.

The LiF bicrystals were cut along a plane perpendicular to the crystal growth direction with a thin diamond blade in a low speed crystal saw. Test specimens were cut so that the grain boundary was transverse across the mid-section of the specimen as indicated in Fig. 2a. Triangular shaped specimens were cut with a crystal saw and were lightly etched with a very dilute solution of ferric chloride in distilled water (10^{-4} molal solution) to reveal the grain boundary [12]. The triangular geometry of the specimen was used so as to make the stress at the tip of the crack to be relatively insensitive to crack length [13].

A schematic drawing of the test fixture used for measuring the fracture load is shown in Fig. 2b. It consists of a screw-driven hardened steel wedge (30°), which can be driven slowly into a notched specimen, and a pre-calibrated

0022–2461/83 $03.00 + .12

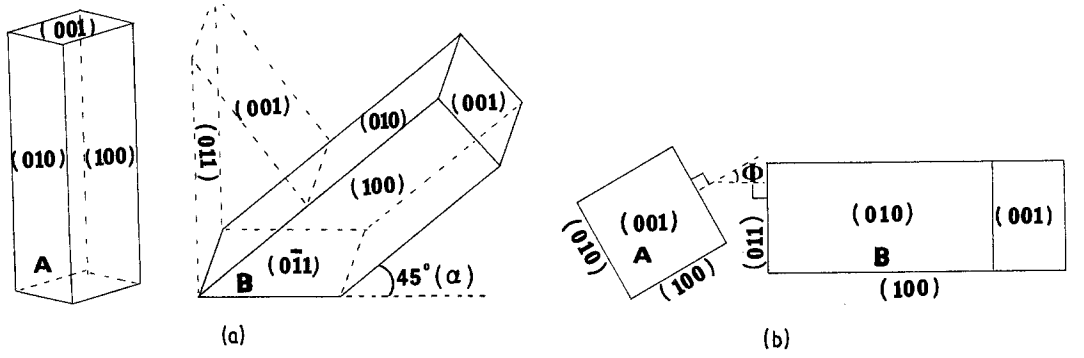

Figure 1 Seed setting used for bicrystal growth [Seed tilt = α (45°), seed rotation = ϕ]. (a) Schematic drawing, and (b) View along growth direction.

load cell for measuring fracture load. The etched triangular specimens were bisected by the crack initiated at the notch. Tensile components of fracture loads were calculated from the fracture loads applied by the screw-driven wedge. The crack paths were observed by an optical microscope with a long focal length objective lens.

Fracture surface energies for primary and secondary cleavage, and grain boundary fracture were measured by using the method developed by Davidge and Tappin [14].

3. Results

Cracks initiated from notch, grew along the (1 0 0) primary cleavage plane in crystal A and propagated along the grain boundary, or across the grain boundary into the crystal B. The crack paths were dictated according to the relative crystallographic and grain boundary orientations. Using optical micrographs of the fractured specimens, crack paths were analysed. Micrographs presented in Figs. 3a, b and c are representative transcrystalline fracture propagation in grain B by primary cleavage. Fig. 3d illustrates a condition under which transcrystalline crack propagation occurs by secondary cleavage. Examples of intercrystalline fracture are presented in Figs. 4a and b. When ϕ values are close to the critical angle ($\phi = 54.5°$) primary and secondary cleavage occurred simultaneously as shown in Fig. 5. Crack propagation through boundaries with twist character necessitates the formation of cleavage steps in the adjoining grain. Some typical pictures of the cleavage steps observed in crystal B are shown in Fig. 6.

In the case of intercrystalline crack propagation, fracture load is a function of the θ values. To illustrate the relation between fracture loads and θ, some experimental results are plotted in Figs. 7a and b for two different ϕ values. Fracture load for intercrystalline fracture increases as the angle θ increases. Likewise, in the case of transcrystalline crack propagation, fracture load is a function of ϕ values. From the curves shown in

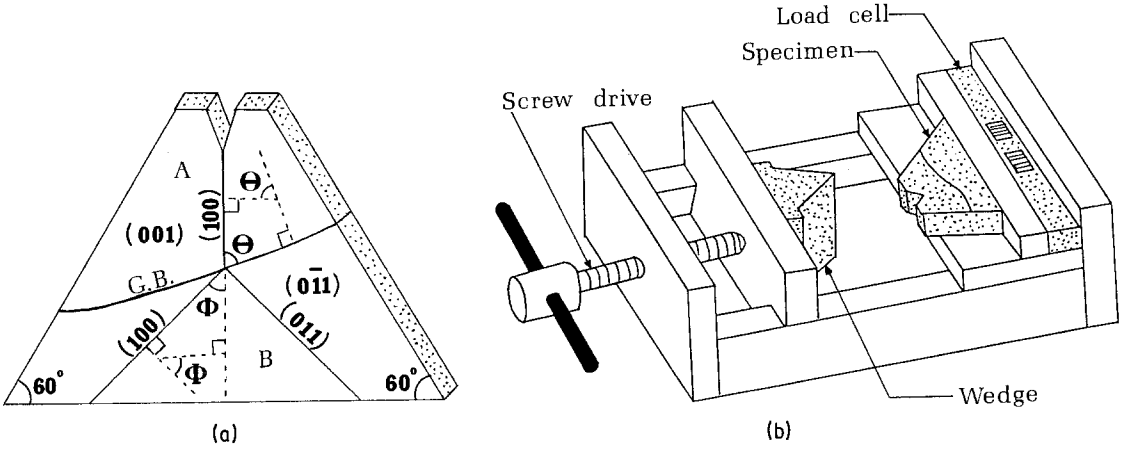

Figure 2 Schematic drawings of (a) specimen geometry, and (b) test fixture (G.B. represents the grain boundary).

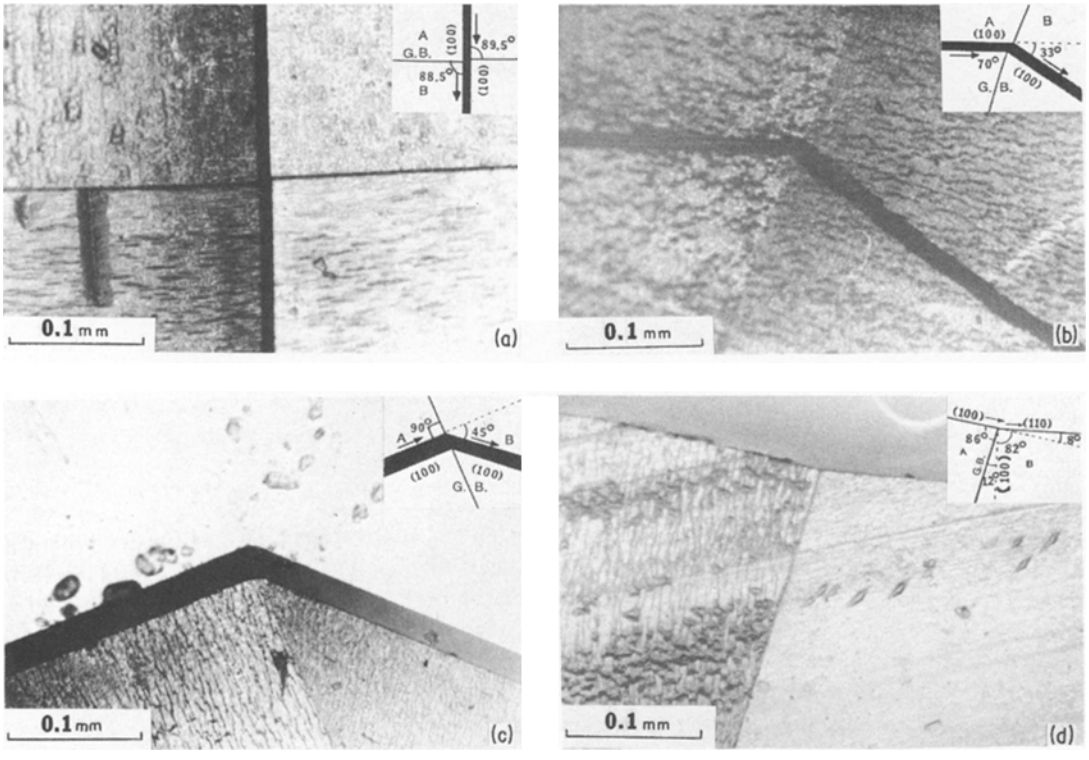

Figure 3 Transcrystalline crack propagation in adjoining crystal (B) along primary and secondary cleavage planes. (a) Primary cleavage, θ: 89.5°, ϕ: 1°, α: 45°, (b) primary cleavage, θ: 70°, ϕ: 33°, α: 45°, (c) primary cleavage, θ: 90°, ϕ: 45°, α: 45° and (d) secondary cleavage, θ: 86°, ϕ: 82°, α: 45°.

Figs. 7c and d, the fracture load for transcrystalline fracture can be observed to increase as the misorientation angle ϕ increases, when θ remains constant.

4. Discussion

4.1. Direction of crack propagation

The brittle fracture of a single crystal occurs when the resolved normal stress reaches a critical value. The critical normal stress, σ_c, for brittle fracture is

$$\sigma_c = \frac{P}{A}\cos^2\beta \qquad (1)$$

where P is the fracture load, A is the cross-sectional area of a plane normal to the tensile axis, and β is the angle between the tensile axis and the normal to the fracture plane [15, 16]. This equation represents Sohncke's Normal Stress Law for the brittle fracture of cubic ionic crystals. The model used in this discussion is an extension

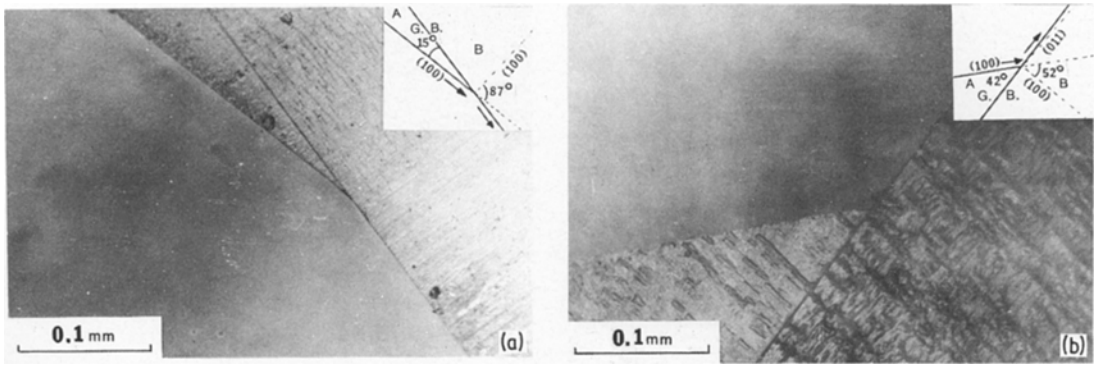

Figure 4 Intercrystalline crack propagation; (a) θ: 42°, ϕ: 52°, α: 45° and (b) θ: 15°, ϕ: 87°, α: 45°.

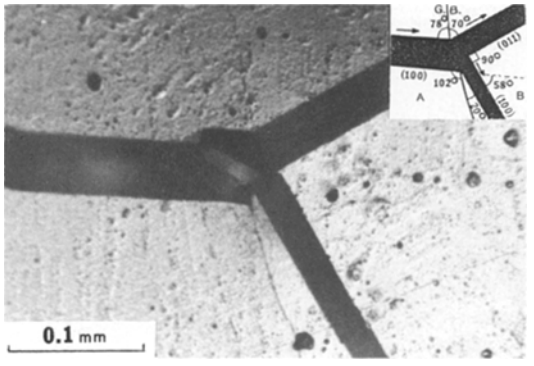

Figure 5 Crack branching on propagation of crack through grain boundary. (Primary and secondary cleavage.) θ: 78°, ϕ: 58°, α: 45°.

of this law. As a consequence, when the crack reaches the grain boundary the mode of fracture in the second grain is that for which the resolved normal stress for fracture is reached first.

The specimens were cut and loaded so as to propagate the crack along the primary cleavage plane in crystal A. Based on the crystal structure of LiF and seed setting, the bicrystal specimens had one potential primary cleavage plane, (1 0 0), and one potential secondary cleavage plane (0 1 1), along which the crack could propagate in crystal B when a (1 0 0) cleavage crack in crystal A reaches the grain boundary.

When a crack tip approaches the grain boundary, crack propagation can occur by one of the following four modes; (i) intercrystalline fracture, (ii) transcrystalline fracture along the primary cleavage plane, (iii) transcrystalline fracture along the secondary cleavage plane, or (iv) fracture along the secondary cleavage plane existing in the crystal containing the initial crack. Crack propagation in a given mode will occur depending on which fracture plane the resolved normal stress first reaches the fracture stress of that plane. The following four equations correspond to the four fracture modes listed above, respectively:

$$\sigma_{cp1} = \sigma_g \cos^2\phi \quad (2)$$

$$\sigma_{cp2} = \sigma_g \cos^2(90° - \phi) \quad (3)$$

$$\sigma_{gb} = \sigma_g \cos^2\theta \quad (4)$$

and

$$\sigma_{cp2.A} = \sigma_g \cos^2 45°, \quad (5)$$

where σ_g is the tensile stress at the grain boundary due to the opening crack, σ_{cp1} is the fracture stress of the primary cleavage plane, σ_{cp2} is the fracture stress of the secondary cleavage plane, σ_{gb} is the fracture stress of the grain boundary, and $\sigma_{cp2.A}$ is the fracture stress of the secondary cleavage plane existing in crystal A.

The critical normal stress is related to the surface energies of the cleavage planes and grain boundary. Thus, depending upon the relative crystallographic and grain boundary orientations, and according to the conditions of the stress concentration, the direction of crack propagation is determined.

The effective surface energy (γ_s) used for this

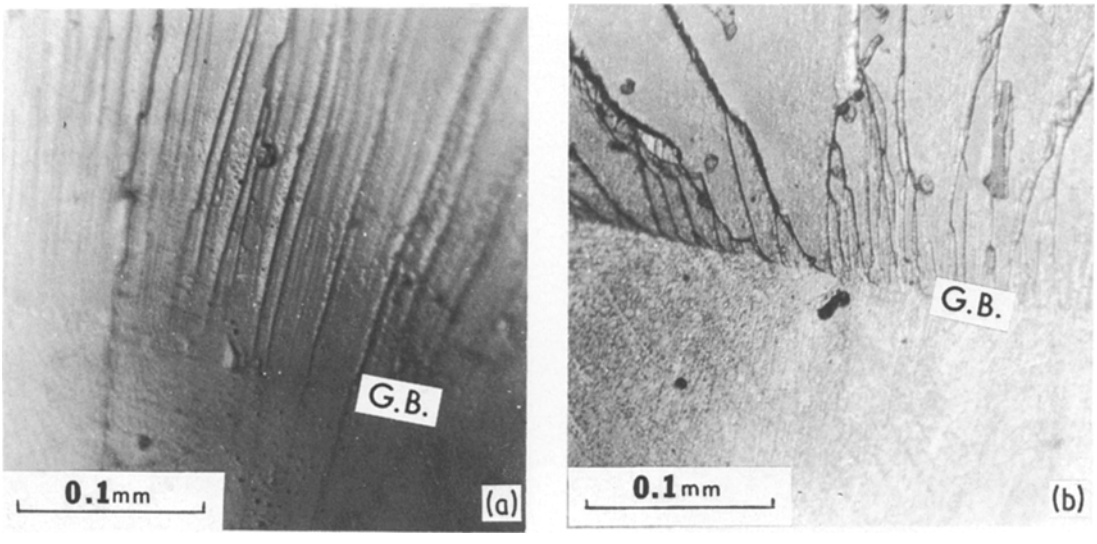

Figure 6 Cleavage steps formed by crack passage through grain boundary. (a) θ: 88.5°, ϕ: 11.5°, α: 45° and (b) θ: 36°, ϕ: 42°, α: 45°.

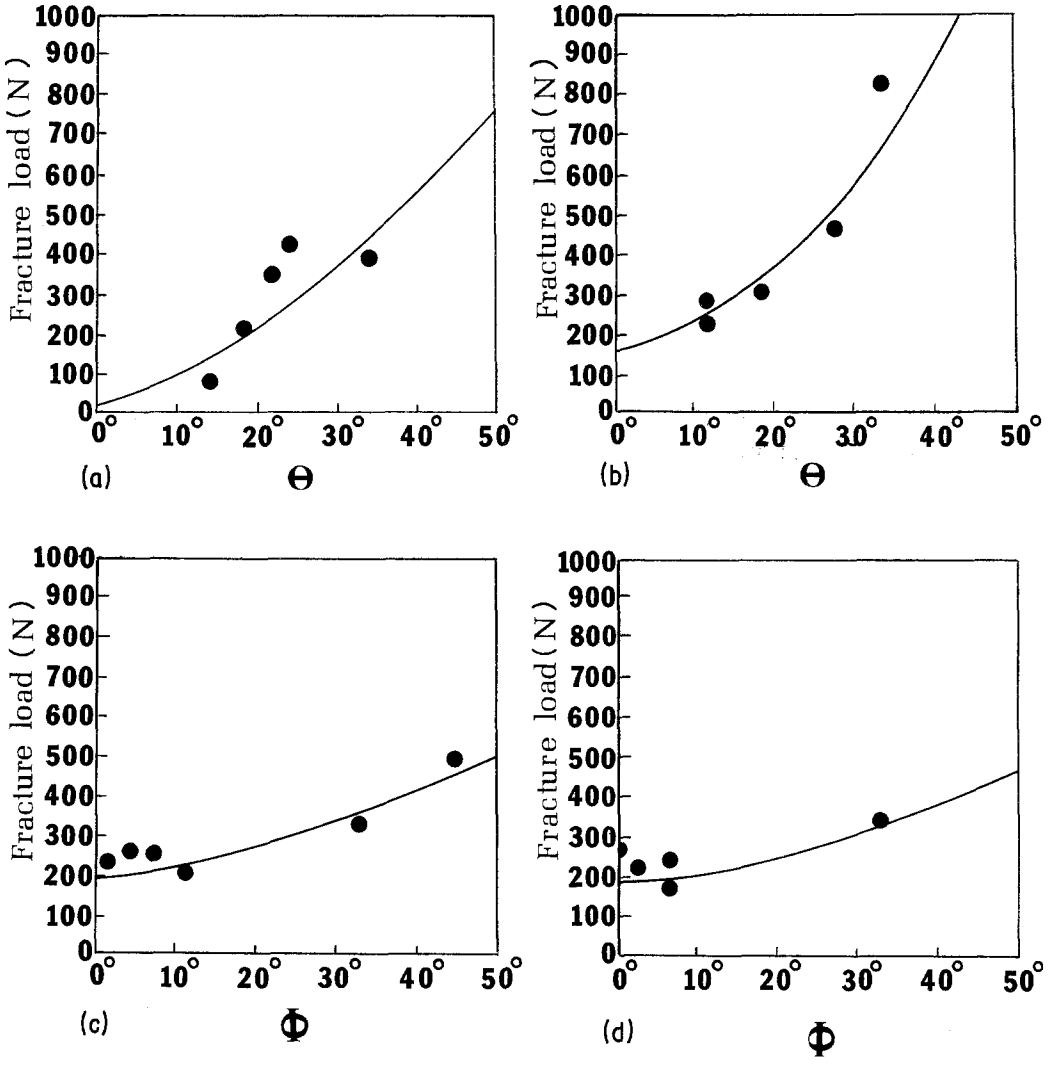

Figure 7 Relation between fracture load and misorientation angles. (a) $86° \leqslant \phi \leqslant 87°$, (b) $80° \leqslant \phi \leqslant 82°$, (c) $86° \leqslant \theta \leqslant 90°$ and (d) $83° \leqslant \theta \leqslant 85°$.

analysis was determined by the notched-bar three-point bending test using the values of the maximum fibre stress at fracture, namely, the modulus of rupture (σ_F), the notch depth (c), and the Young's modulus (E) [14]. When the notch depth is small compared with the beam depth, the effective surface energy is given by

$$\gamma_s = \frac{(1-\nu^2)\pi\sigma_F^2 c}{2E} \quad (6)$$

where ν is Poisson's ratio [14]. The experimentally measured values of the surface energy are listed in Table I. These values are averages based on six tests for each condition. Further, the calculated fracture stress, σ_f, is related to γ_s by the equation

TABLE I Experimental values of surface energy and corresponding calculated fracture stress of LiF crystals for various fracture modes

Fracture plane	Surface energy (Jm^{-2})	Calculated fracture stress (Nm^{-2})
Primary cleavage plane	0.52	1.15×10^{10}
Secondary cleavage plane	2.00	2.25×10^{10}
Grain boundary	0.94	1.54×10^{10}

$$\sigma_f = \left(\frac{E\gamma_s}{a_0}\right)^{1/2} \quad (7)$$

where a_0 is lattice constant [17]. By substituting the constants of LiF ($E = 1.02 \times 10^{11}\,\mathrm{Nm}^{-2}$, $a_0 = 4.027 \times 10^{-10}\,\mathrm{m}$) in the above equation, the fracture stress needed for separation along various planes were calculated. As an approximation, variations in E and a_0 for various fracture surfaces are neglected since the bicrystals had grain boundaries with various misorientations. Variations in γ of the grain boundary, due to the various relative crystallographic orientations of grains A and B, are also neglected so as to simplify the computations. The calculated fracture stresses are listed in Table I.

From these experimental results,

$$\sigma_{cp1} = 0.746\,\sigma_{gb} \quad (8)$$

$$\sigma_{cp2} = 1.461\,\sigma_{gb} \quad (9)$$

$$\sigma_{cp1} = 0.511\,\sigma_{cp2} \quad (10)$$

and

$$\sigma_{cp2.A} = 1.461\,\sigma_{gb}. \quad (11)$$

The angle between (1 0 0) and (1 $\bar{1}$ 0) planes in crystal A is 45°. Equations 4, 5 and 11, when combined together, provide the condition for secondary cleavage in crystal A;

$$\sigma_g \cos^2 45^\circ = 1.461\,\sigma_g \cos^2\theta \quad (12)$$

i.e. $\theta = 54.2^\circ$. Crack propagation along the secondary cleavage plane existing in crystal A occurs when $\theta > 54.2^\circ$. But, if $\theta > 54.2^\circ$ crystal A does not contain a (1 $\bar{1}$ 0) plane in the suitable direction for crack propagation. Therefore, such a crack propagation mode is impossible.

From Equations 2, 4 and 8 the condition for transcrystalline fracture along the primary cleavage plane is $\cos^2\phi < 0.7437\cos^2\theta$ and the condition for intercrystalline fracture is $\cos^2\phi > 0.7437\cos^2\theta$. These conditions are plotted as curve I in Fig. 8.

Likewise, from Equations 3, 4 and 9 the condition for transcrystalline fracture along the secondary cleavage plane is

$$\sigma_g \cos^2(90^\circ - \phi) < 1.461\,\sigma_g \cos^2\theta \quad (13)$$

and the condition for intercrystalline fracture is

$$\sigma_g \cos^2(90^\circ - \phi) > 1.461\,\sigma_g \cos^2\theta. \quad (14)$$

These conditions are plotted as curve II in Fig. 8. The orientation of the grain boundary does not have any effect on the transcrystalline cleavage along the primary cleavage plane or secondary cleavage plane in crystal B. So, from Equations 2, 3 and 10 the condition for crack propagation along the primary cleavage plane is $\cos^2\phi > 0.511\cos^2(90^\circ - \phi)$ and for the secondary cleavage plane is $\cos^2\phi < 0.511\cos^2(90^\circ - \phi)$. These conditions are plotted as curve III in Fig. 8. Thus, by superimposing the crack propagation conditions, the misorientation conditions for different crack propagation modes at a grain boundary can be obtained as shown in Fig. 8.

Curve I of Fig. 8 shows the various combinations of critical angles (θ and ϕ) at which intercrystalline fracture and transcrystalline cleavage along the primary cleavage plane could occur simultaneously. Curve II of Fig. 8 shows the various combinations of critical angles (θ and ϕ) at which intercrystalline fracture and transcrystalline cleavage along the secondary cleavage plane could occur simultaneously. The critical value of ϕ is 54.5°, at which transcrystalline cleavage could occur along the primary cleavage plane or along the secondary cleavage plane.

Thus, in the zone "TR.1." in Fig. 8, only transcrystalline cleavage along the primary cleavage plane could occur. In the zone "TR.2." only transcrystalline cleavage along the secondary cleavage plane could occur. In the zone "IN." only intercrystalline fracture occurs. But at the critical point, which is the junction of the three curves, the three possible modes of crack propagation could occur simultaneously. As indicated earlier, secondary cleavage in crystal A does not occur for the given specimen geometry.

Experimental results are also incorporated in Fig. 8 by placing different markers to indicate various fracture modes as a function of the misorientation angles. As can be seen from this figure, the experimental observations fully conform with the predictions of the simple model considered for the analysis. For example, crack propagation modes presented in Fig. 3 through 5 fully agree with the predictions of the model.

5. Summary

The fracture mode of bicrystals depends on the misorientation angles. Observations made with LiF bicrystals having specific misorientation angles can be summarized as follows:

1. When angle ϕ is smaller than 30.4°, only primary cleavage fracture occurs regardless of the value of the angle of relative grain boundary

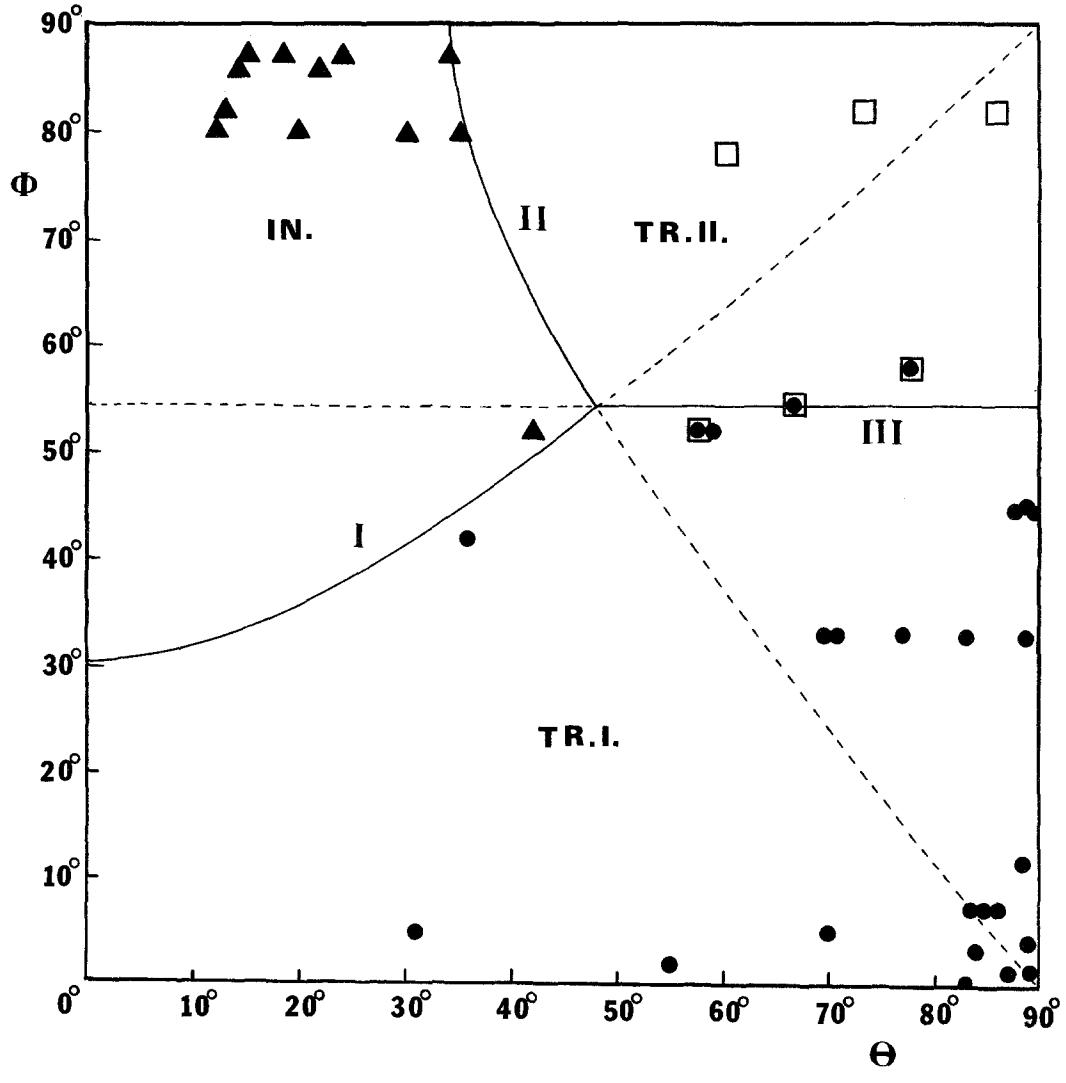

Figure 8 Crack propagation mode for various θ and ϕ. Experimental points are indicated in the same plot. ▲ intercrystalline fracture (experimental), • transcrystalline (primary) cleavage (experimental), □ transcrystalline (secondary) cleavage (experimental), IN. intercrystalline propagation zone, TR.1. transcrystalline (primary) propagation zone and TR.2. transcrystalline (secondary) propagation zone. (■ indicates that transcrystalline (primary) cleavage and transcrystalline (secondary) cleavage occurred simultaneously in the same specimen as shown in Fig. 5).

orientation (θ). Similarly for values of θ from 47.6 to 90°, primary cleavage always occurs provided ϕ is less than 54.5°. For the values of θ ranging from 0 to 47.6°, primary cleavage occurs provided ϕ is smaller than the corresponding critical angles, ranging from 30.4 to 54.5°. When the angle ϕ is larger than the critical angle, intercrystalline fracture also occurs provided the θ value is smaller than the critical angle at which intercrystalline fracture and secondary cleavage can occur simultaneously. Intercrystalline and transcrystalline fracture and secondary cleavage fracture occur simultaneously at the critical angles.

2. The load required to fracture bicrystals increases when the misorientation angles increase.

3. The fracture mode can be predicted from the calculated resolved normal stresses on potential fracture planes, and the corresponding fracture strength of these planes.

References

1. N. FAT-HALLA, T. TAKASUGI and O. IZUMI, *J. Mater. Sci.* 13 (1978) 2462.
2. A. W. BOWEN, *Acta Metall.* 23 (1975) 1401.
3. G. MIMA, F. INOKO and K. ATAGI, *J. Jpn. Inst. Met.* 42 (1978) 887.
4. A. H. HEUER, *J. Amer. Ceram. Soc.* 52 (1969) 510.

5. A. G. EVANS and L. J. GRAHAM, *Acta Metall.* **23** (1975) 1303.
6. A. R. C. WESTWOOD, *Phil. Mag.* **6** (1961) 195.
7. P. P. GILLIS and J. J. GILMAN, *J. Appl. Phys.* **35** (1964) 647.
8. J. J. GILMAN, *Acta Metall.* 7 (1959) 608.
9. C. O. HULSE, S. M. COPPLEY and J. A. PASK, *J. Amer. Ceram. Soc.* **46** (1963) 317.
10. J. J. GILMAN, C. KNUDSEN and W. P. WALSH, *J. Appl. Phys.* **29** (1958) 601.
11. J. J. GILMAN, *AIME Trans.* **209** (1957) 449.
12. J. J. GILMAN and W. G. JOHNSTON, "Dislocations and Mechanical Properties of Crystals" (Wiley, New York, 1956) p. 116.
13. W. D. BASCOM, R. L. COTTINGTON, R. L. JONES and P. PEYSER, *J. Appl. Polym. Sci.* **19** (1975) 2545.
14. R. W. DAVIDGE and G. TAPPIN, *J. Mater. Sci.* **3** (1968) 165.
15. L. SOHNCKE, *Poggendorfs Ann.* **137** (1869) 177.
16. E. SCHMID and I. W. BOAS, "Plasticity of Crystals" (Chapman and Hall, London 1950) p. 169, p. 241.
17. W. D. KINGERY, H. K. BOWEN and D. R. UHLMANN, "Introduction to Ceramics" (John Wiley and Sons, New York, 1976) p. 784.

Received 10 August
and accepted 19 November 1982